Am J Physiol Endocrinol Metab 319: E1061–E1073, 2020.
First published October 12, 2020; doi:10.1152/ajpendo.00235.2020.

RESEARCH ARTICLE

Diet during early life defines testicular lipid content and sperm quality in adulthood

Luís Crisóstomo,[1,2,3] Romeu A. Videira,[1,4] Ivana Jarak,[1,4] Kristina Starčević,[5] Tomislav Mašek,[6] Luís Rato,[4] João F. Raposo,[7,8] Rachel L. Batterham,[9] Pedro F. Oliveira,[10] and Marco G. Alves[1]

[1]*Department of Microscopy, Laboratory of Cell Biology, and Unit for Multidisciplinary Research in Biomedicine, Institute of Biomedical Sciences Abel Salazar, University of Porto, Porto, Portugal;* [2]*Department of Genetics, Faculty of Medicine of the University of Porto, Porto, Portugal;* [3]*i3S - Instituto de Investigação e Inovação em Saúde, University of Porto, Porto, Portugal;* [4]*Faculty of Health Sciences, University of Beira Interior, Covilhã, Portugal;* [5]*Department of Chemistry and Biochemistry, University of Zagreb, Faculty of Veterinary Medicine, Zagreb, Croatia;* [6]*Department of Animal Nutrition and Dietetics, University of Zagreb, Faculty of Veterinary Medicine, Zagreb, Croatia;* [7]*NOVA Medical School, New University Lisbon, Lisbon, Portugal;* [8]*Associação Protectora dos Diabéticos de Portugal, Diabetes Portugal, Lisbon, Portugal;* [9]*Centre for Obesity Research, Rayne Institute; Centre for Weight Management and Metabolic Surgery and National Institute of Health Research, University College London, London, United Kingdom; and* [10]*Unidade de Investigação em Química Orgânica, Produtos Naturais e Agroalimentares (QOPNA) and Laboratório Associado para a Química Verde | Associated Laboratory for Green Chemistry (LAQV), Department of Chemistry, University of Aveiro, Aveiro, Portugal*

Submitted 19 May 2020; accepted in final form 30 September 2020

Crisóstomo L, Videira RA, Jarak I, Starčević K, Mašek T, Rato L, Raposo JF, Batterham RL, Oliveira PF, Alves MG. Diet during early life defines testicular lipid content and sperm quality in adulthood. *Am J Physiol Endocrinol Metab* 319: E1061–E1073, 2020. First published October 12, 2020; doi:10.1152/ajpendo.00235.2020.— Childhood obesity is a serious concern associated with ill health later in life. Emerging data suggest that obesity has long-term adverse effects upon male sexual and reproductive health, but few studies have addressed this issue. We hypothesized that exposure to high-fat diet during early life alters testicular lipid content and metabolism, leading to permanent damage to sperm parameters. After weaning (*day 21* after birth), 36 male mice were randomly divided into three groups and fed with a different diet regimen for 200 days: a standard chow diet (CTRL), a high-fat diet (HFD) (carbohydrate: 35.7%, protein: 20.5%, and fat: 36.0%), and a high-fat diet for 60 days, then replaced by standard chow (HFD_t). Biometric and metabolic data were monitored. Animals were then euthanized, and tissues were collected. Epididymal sperm parameters and endocrine parameters were evaluated. Testicular metabolites were extracted and characterized by 1H-NMR and GC-MS. Testicular mitochondrial and antioxidant activity were evaluated. Our results show that mice fed with a high-fat diet, even if only until early adulthood, had lower sperm viability and motility, and higher incidence of head and tail defects. Although diet reversion with weight loss during adulthood prevents the progression of metabolic syndrome, testicular content in fatty acids is irreversibly affected. Excessive fat intake promoted an overaccumulation of proinflammatory n-6 polyunsaturated fatty acids in the testis, which is strongly correlated with negative effects upon sperm quality. Therefore, the adoption of high-fat diets during early life correlates with irreversible changes in testicular lipid content and metabolism, which are related to permanent damage to sperm quality later in life.

high-fat diet; early-life obesity; diet intervention; lipidomics; male fertility

INTRODUCTION

The fast and global increase of overweight/obesity in recent decades has led the World Health Organization to declare it the "Epidemic of the XXI Century" (72). Excessive fat deposition has been associated with the onset of noncommunicable diseases, particularly Type 2 diabetes (T2DM) (22). Consumption of energy-dense, high-fat diet (HFD) and low physical activity are two major drivers of the obesity epidemic (22). In developed countries, consumption of energy-dense foods occurs at an ever-younger age (41). Childhood obesity rates continue to soar worldwide, with obesity-associated comorbidities occurring at a younger age (33, 71). Concurrently, concerns on the impact of excessive adiposity and T2DM on sperm quality and fertility outcomes have been raised (14, 42, 51). Although there are not many studies demonstrating the impact of fat-rich diets in sperm quality, men attending fertility centers are often advised to lose weight and adopt a balanced diet. Unlike the other lifestyle interventions such as physical activity (62), the effectiveness of dietary intervention in recovering normal sperm quality, or its positive effects on testicular metabolism, has never been demonstrated (64).

Normal male reproductive function requires a well-orchestrated balance of endocrine and metabolic factors to secure proper energy flow toward meiosis and cellular remodeling of differentiating germ cells (55). In this regard, testicular lipid dynamics are crucial, not only as energy substrates, but also as structural elements of the future sperm cells. Moreover, mitochondrial function and antioxidant defenses are crucial for providing energy for spermatogenesis and sperm motility, while avoiding oxidative damage, which can critically compromise cell function. Previously, we have shown that HFD during early life causes irreversible changes in testicular metabolism, even after reversion, and those changes are correlated to defects in sperm motility, viability, and morphology (12). The relevance of fatty acids in testicular physiology has been reported, especially the repercussions for spermatogenesis (20, 28, 37, 57).

Correspondence: M. G. Alves (alvesmarc@gmail.com).

We hypothesize that the adoption of HFDs affects testicular lipid dynamics, resulting in poor sperm quality. We further address whether an HFD early in life can irreversibly affect sperm quality later in life, due to testicular lipid dysmetabolism, even after diet intervention in early adulthood. We have performed our study in a rodent model. Biometry, glucose homeostasis, endocrine function, testicular antioxidant system, testicular bioenergetics, and sperm parameters were assessed. We have further performed a multivariate analysis supported by targeted metabolomics and lipidomics, based on semiquantitative GC-MS and ^{1}H-NMR, to determine changes in testicular lipid metabolism.

MATERIALS AND METHODS

Animal model. Mus musculus C57BL6/J male mice (n = 36) were randomly divided into three groups after weaning (21–23 days): control (CTRL) (n = 12), HFD (n = 12), and transient HFD (HFD_t) (n = 12). All mice were generated from normoponderal males and females and were subjected to the same random in utero stimuli, although generated from different litters. Briefly, CTRL group mice were fed with a standard chow (no. F4031, BioServ: carbohydrate: 61.6%, protein: 20.5%, and fat: 7.2–16.3% kcal). The HFD group mice received an HFD (no. F3282, BioServ: carbohydrate: 35.7%, protein: 20.5%, fat: 36.0–59.0% kcal) for 200 days after weaning. HFD_t group mice were fed with an HFD (no. F3282; BioServ, Flemington, NJ) for 60 days and then switched to standard chow (no. F4031, BioServ). At 120 days postweaning, mice were randomly assigned to a normoponderal female, in mating pairs, 6 h/day, for seven consecutive days, for breeding. During this period, female breeders were maintained on the same standard diet. Mating pairs had no access to water or food during mating (6 h). Reproductive success rate, litter size, and litter male-to-female ratio were assessed. Animals were killed by cervical dislocation 200 days after weaning, and tissues were collected for further analysis. Total body weight, water, and food intake were monitored weekly until euthanization. The animal model is compliant with the ARRIVE guidelines and was licensed by the Portuguese Veterinarian and Food Department (0421/000/000/2016).

Endocrine and metabolic function. Fasting glycemia was measured before euthanization (200 days postweaning), after overnight fast (8 h), using a glucometer (One Touch Ultra Lifescan-Johnson, Milpitas, CA) by collecting a drop of blood from the tail vein. Blood was then collected by cardiac puncture and centrifuged at 1500 g, 4°C, for 10 min to collect the serum. Serum insulin was quantified using a rat/mouse insulin ELISA assay (EZRMI-13K; Millipore). Glucose homeostasis was evaluated according to the homeostasis model assessment 2 (HOMA2) scores (30), using the HOMA2 calculator (University of Oxford, UK). Disposition index (DI) was calculated as suggested by Caumo et al. (9). Similarly, follicle-stimulating hormone (FSH), leutinizing hormone (LH), 17β-estradiol, and testosterone were quantified in the purified serum using ELISA kits (respectively, ENZ-KIT108-0001, ENZ-KIT107-0001, ADI-900-174 and ADI-900-176; Enzo Life Sciences).

Evaluation of epididymal sperm parameters. Epididymides were isolated and placed in prewarmed (37°C) Hank's balanced salt solution (HBSS) at pH 7.4, and then minced with a scalpel blade. Then the suspension was incubated for 5 min (37°C). Sperm parameters were evaluated as previously described (12, 53). Sperm motility was calculated as the average proportion of motile sperm in 10 random microscope fields, observing a drop of sperm suspension on a warmed slide (37°C) using an optical microscope (×100 magnification). Epididymal sperm concentration was determined using a Neubauer counting chamber and an optical microscope (×400 magnification) in a diluted sperm suspension (1:50 in HBSS). Sperm viability and morphology were assessed in differently stained epididymal sperm smears, counting 333 spermatozoa in random fields using an optical microscope (×400 magnification). Sperm viability smears were stained with eosin-nigrosin (29), as membrane-compromised spermatozoa stain pink. Sperm morphology smears were stained with Diff-Quick (Baxter Dale Diagnostics AG, Dubinger, Switzerland). Sperm morphology categories were mutually exclusive, i.e., spermatozoa displaying more than one defect were assigned according to the most serious defect category (decapitated > pinhead > flattened head > bent neck > coiled tail) (29).

NMR spectroscopy. A combined extraction of polar and nonpolar metabolites from testicular tissue was performed as previously described (2, 12). Testes were washed with saline and decapsulated before metabolite extraction to minimize contamination by blood metabolites. The aqueous phase containing polar water-soluble metabolites was lyophilized and analyzed by ^{1}H-NMR spectroscopy, as described by Jarak et al. (25). Lipid metabolites were identified by comparing recorded spectra with reference spectra and the Human Metabolome Database (69), and according to Metabolomics Standards Initiative guidelines for metabolite identification (65). Identification levels are indicated in Supplemental Table S1 (all Supplemental material is available at https://doi.org/10.6084/m9.figshare.12302171). ^{1}H spectra were processed using previously described methods (25). Obtained peak areas were normalized by the total spectral area and analyzed by univariate analysis. Areas were obtained using AMIX software (Bruker BioSpin, Rheinstetten, Germany) and expressed as arbitrary units defined by the software.

GC-MS analysis. Fatty acid methyl esters of total lipids were obtained by base-catalyzed transmethylation (2 M KOH in methanol) in the presence of nonadecanoic fatty acid (C19:0), used as the internal standard. The obtained hexane fatty acid methyl esters solution was analyzed by gas chromatography using a Shimadzu GC–MS QP2010 UltraGas Chromatograph Mass Spectrometer (Shimadzu, Kyoto, Japan), equipped with a capillary column BPX70 (0.25-mm internal diameter, 0.25-μm film thickness, 30-mlength, SGE, Austin, TX). The injector temperature was 250°C, and 1 μl of each sample was injected with a split ratio of 1:80. Helium was used as the carrier gas, and the linear velocity was 35 cm/s. The initial column temperature was 155°C, followed by a heating rate of 1°C/min up to 170°C, 4°C/min up to 220°C and 40°C/min until reaching 250°C, maintained for 5 min. Linear velocity was 35 cm/s, interface temperature: 250°C, ion source temperature: 225°C, mass range: 45–500 and event time: 0.3 s. All of the experimental measurements were repeated three times, and the average values were reported. Fatty acids were identified by retention time and fragmentation profile and were quantified by the internal standard procedure. Results were expressed as a percentage of total fatty acids.

Lipid peroxidation, activity of antioxidant enzymes, and activity of mitochondrial enzyme complexes. A single testis from each animal was homogenized in 2 mL of ice-cold extraction buffer [160 mM sucrose, 10 mM Tris·HCl, at pH 7.4], supplemented with a protease inhibitor cocktail (no. B14001, Bimake, Munich, Germany) (1:10, p/v)] using a glass-Teflon Potter Elvejhem (Kimble, Millville, NJ). The resulting homogenate was split into two fractions: one was used for adenine nucleotide (ATP, ADP, and AMP) extraction and quantification by high-performance liquid chromatography (HPLC), as described previously (40); the other was fractionated by differential centrifugation to obtain a mitochondria-free cytosolic fraction and a mitochondria-enriched fraction, as described previously (38, 40). The final protein content of each fraction was determined by the BCA method (61). The mitochondria-enriched fraction was used to assess the activity of the mitochondrial enzymes (complexes I, II, IV, and V and citrate synthase), while the mitochondria-free cytosolic fraction was used to evaluate the activity of the enzymes of the antioxidant defense system [catalase (CAT), copper-zinc superoxide dismutase (SOD), glutathione peroxidase (GPx), glutathione-disulfide reductase (GSR)] and to assess the levels of lipid peroxidation.

CAT activity was polarographically determined following oxygen production resulting from H_2O_2 decomposition using a Clark-type oxygen electrode (Hansatech, Norfolk, UK) (13). SOD, GPx and GSR activities were evaluated in 96-well plates, at 37°C, as described

previously (46). The reaction was conducted in 930 μL of 100 mM potassium phosphate buffer (100 mM KH_2PO_4, 5 mM EDTA, pH 7.4) with 50 μL of testicular cytosol extract, and initiated by adding 20 μL of H_2O_2 (2 mM). CAT activity was expressed in nanomoles O_2 per minute per milligram protein.

SOD activity was evaluated by mixing 50 μl testicular cytosolic fraction with 170 μl potassium phosphate buffer, supplemented with 2 mM nitro blue tetrazolium (NBT), and 0.05 U xanthine oxidase (no. X1875-10UN, Sigma-Aldrich/Merck KGaA, Darmstadt, Germany). After addition of 10 μL hypoxanthine (2 mM), absorbance at 560 nm was measured every 20 s for 5 min. Results were expressed as units per minute per milligram of protein, where U is the enzyme activity that inhibited the reduction of NBT to blue formazan by 50%.

Glutathione reductase (GR) activity was evaluated by the rate of NADPH oxidation associated with the reduction of GSSG. Assays were carried out in 170 μL potassium phosphate buffer, supplemented with 10 mM NADPH and 10 mM GSSG. After adding 300 μL of testicular cytosolic fraction, NADPH oxidation was recorded by the fluorescence decrease at 450 nm (excitation: 360 nm) every 20 s for 5 min. NADPH oxidation not associated with GSSG reduction was assessed in assays carried out in the absence of GSSG. GR activity was determined by difference between the rate of NADPH oxidation in the presence and absence of GSSG and expressed in nanomoles per minute per milligram of protein.

GPx activity was evaluated by the rate of NADPH oxidation associated with H_2O_2 reduction. Assays were performed in 170 μL potassium phosphate buffer, supplemented with 10 mM GSH and 1–3U glutathione reductase (no. G3664-500UN, Sigma-Aldrich/Merck KGaA, Darmstadt, Germany), and 50 μL of testicular cytosol fraction. Reaction was initiated by the addition of 10 μL H_2O_2 (0.6 mM), and fluorescence at 450 nm (excitation: 360 nm) was measured every 20 s for 5 min. GPx activity was determined by the rate of NADPH consumption in nanomoles per minute per milligrams of protein.

Testicular lipid peroxidation levels were evaluated by the production of thiobarbituric acid reactive species (TBARS assay). Shortly, 50 μL testicular cytosolic fraction were mixed with 600 μL of reaction solution [thiobarbituric acid 0.38% (m/V), trichloroacetic acid 37% and 2,6-ditertbutyl-4-methylphenol 0.02% (m/V) (38)] and incubated at 95°C for 30 min. Malondialdehyde (MDA) formation was measured by colorimetric methods ($\varepsilon = 156\ mM^{-1}/cm^{-1}$), and results were expressed in nanomoles of MDA per milligram of protein.

Activities of the mitochondrial complexes I, II and IV, and citrate synthase (CS) were assessed, at 37°C, in 96-well plate by adapting previously described protocols (40). CS was determined spectrophotometrically, by monitoring the reduction of DTNB. The reaction mixture consisted of 200 mM Tris·HCl buffer (pH 8.0), 0.02% Triton X-100, 10 M DTNB, 1 mM oxaloacetate, and 20 μL of testicular mitochondrial fraction. The reaction was initiated by adding 0.37 mM acetyl-CoA, and the absorbance at 412 nm was recorded every 30 s for 10 min. CS activity was calculated by DTNB ($\varepsilon = 13.6\ mM^{-1}/cm^{-1}$) reduction rate, determined in the linear range of the plot and expressed as nanomoles per minute per milligram of protein.

Complex I activity was assessed following NADH oxidation. The reaction was performed in a potassium phosphate buffer (25 mM KH_2PO_4, 10 mM $MgCl_2$; pH 7.4) supplemented with 1 mM KCN, 162.5 μM decylubiquinone, 3.0 μM rotenone (or equal volume of buffer) and 20 μL of testicular mitochondrial fraction. The reaction was triggered by the addition of NADH (50 μM), and fluorescence at 450 nm (excitation: 366 nm) was measured every 20 s for 15 min. Complex I activity was determined by the difference between NADH oxidation rate in rotenone-inhibited wells and noninhibited wells. This value was expressed in nanomoles of NADH per minute per milligram.

Complex II activity was assessed monitoring 2,6-dichlorophenolindo-phenol (DCPIP) reduction at 600 nm ($\varepsilon = 20.7\ mM^{-1}\cdot cm^{-1}$) in a potassium phosphate buffer, supplemented with 2 mM KCN, 6.5 μM rotenone, 6.5 μM antimycin A, 0.05 mM DCIP, 0.1 mM decylubiquinone, and 20 μL of testicular mitochondrial fraction. Negative control wells were further supplemented with 0.5 mM oxaloacetate (complex II inhibitor). The reaction was initiated by adding 20 mM succinate and absorbance measure every 30 s for 20 min. Complex II activity was expressed as the DCPIP reduction rate (corrected for spontaneous reduction) in nanomoles of DCPIP per minute per milligram protein.

Complex IV activity was evaluated by the cytochrome-*c* (CytC) oxidation rate. CytC (50 mM) was fully reduced by the addition of small volumes of saturated sodium dithionite solution. CytC oxidation reaction was performed in extraction buffer, supplemented with 3 μM rotenone, 0.1 μM antimycin A (inhibitor of complex III), 2 mM KCN (specific inhibitor of complex IV), or equal volume of buffer, and 20 μL of testicular mitochondrial fraction. The reaction was initiated by adding 15 μM reduced CytC, and the absorbance at 550 nm was recorded every 15 s for 5 min. Complex IV activity was calculated by CytC ($\varepsilon = 29.5\ mM^{-1}\cdot cm^{-1}$) oxidation rate, corrected by the spontaneous oxidation rate obtained in the KCN-inhibited wells, and expressed as nanomoles of CytC per minute per milligram of protein.

Maximal activity of the mitochondrial complex V was measured using a MitoCheck Complex V activity assay kit (Cayman Chemical, Ann Arbor, MI). All colorimetric and fluorometric readings described in this section were obtained using a Biotek Synergy H1 plate reader (Winooski, VT).

Determination of testicular adenosine nucleotides levels by HPLC. Testicular adenosine nucleotides levels were assessed in a Waters 600 HPLC system (Waters, Milford, MA) equipped with 2487 dual-λ absorbance detector. ATP, ADP, and AMP were separated on a reverse-phase chromatography column (Lichrospher RP-18 HPLC Column, 5-μm particle size, L × I.D. 25 cm × 4.6 mm), using a gradient mobile phase that consisted of phase A (100 mM KH_2PO_4 buffer with 1.2% methanol vol/vol, at pH = 7.0) and phase B (100 mM KH_2PO_4 buffer with 10% methanol vol/vol, at pH = 7.0) The elution program was the following: 100% of A from 0 to 20 min followed by a linear gradient up to 100% of B until 25 min, and from 25 to 28 min down to 0% B (initial conditions). The flow was 1 mL/min, and the column temperature was maintained at 25°C during the run. Chromatograms were recorded at 254 nm, and analyzed using the Waters Millennium32 (Waters, Milford, MA). Peaks were identified by their retention times, comparing them with samples of standard compounds. ATP, ADP, and AMP levels were quantified using standard curves obtained with a serial of known concentrations of each of the adenine nucleotides run on the same day and conditions of the samples. The results were expressed as moles per gram wet tissue.

Statistical and exploratory factor analysis. Different statistical methods were applied depending on the objective and the nature of the analyzed data. Kolmogorov-Smirnoff test was used to test data normality. Whenever normality was ensured, one-way ANOVA with the Tukey post hoc test was set as the default test. Whenever this assumption was violated, extreme values of more than three standard deviations from the mean were omitted. Otherwise, the nonparametric Kruskal-Wallis test was performed, using the Mann-Whitney *U* test as a post hoc test. The overall distribution of sperm defects between groups was further tested using the χ^2 test. The nonparametric Spearman correlation was used to correlate fertility and sperm parameters. The parametric Pearson correlation (*r* coefficients) was used to correlate the different sets of variables in the study (sperm parameters, endocrine and metabolic function, mitochondrial function, bioenergetics, and antioxidant system), after variables were successfully tested for normality using the Kolmogorov-Smirnoff test, and as part of exploratory factor analysis. The correlation strength was classified according to ranks (67). Variables with significant ($P < 0.05$) linear correlation with sperm parameters were then considered for Multivariate Analysis based on principal components analysis (PCA). Although PCA is an unsupervised multivariate method, it was used as a sparse and supervised method considering the variable selection criteria based on linear (Pearson) correlation. Forced factor extraction was performed to extract 2 principal components (PCs), based on the interpretability criterion, and using Varimax with Keiser's normalization as rotation method. Regression factors were used to plot sample distribution

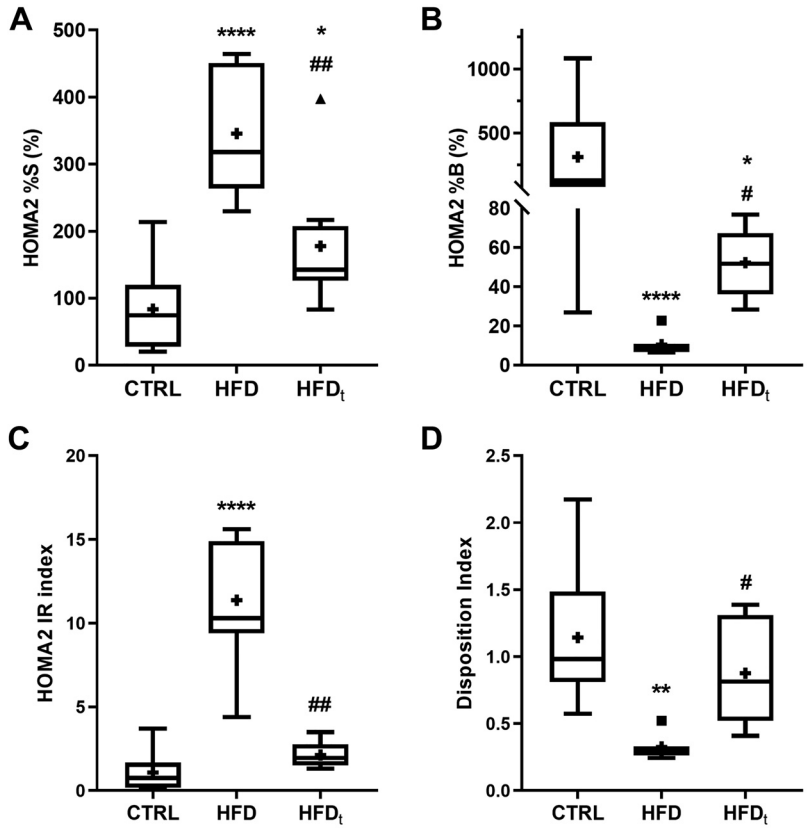

Fig. 1. Homeostasis model assessment 2 (HOMA2) indexes and disposition index of mice fed standard chow (CTRL) or lifelong high-fat diet (HFD) or subjected to diet correction after 60 days (HFD_t). Fasting glycemia and insulin were used as inputs for the interactive HOMA2 calculator (University of Oxford, UK). Results are expressed as Tukey whisker boxes [median, 25th to 75th percentiles ± 1.5 interquartile range (IQR)]. Extreme values are represented individually (■ denotes HFD, high-fat diet; ▲ denotes HFD_t, transient high-fat diet). Data were tested by one-way ANOVA with the Tukey HSD for group comparison. Significance was considered when $P < 0.05$. +Group average. * vs. CTRL. # vs. HFD. *$P < 0.05$; **$P < 0.01$; ****$P < 0.0001$; #$P < 0.05$; ##$P < 0.01$.

in the two-dimensional Euclidean space. All methods were performed using IBM SPSS statistics v25 (Armonk, NY). Independently of the statistical method used, significance was considered whenever $P < 0.05$.

RESULTS

Hormonal balance is not affected by high-fat diets, and glucose homeostasis is recovered after dietary correction. In our previous study (12), we found that dietary switch from a fat-rich diet to a standard chow was able to normalize biometric parameters (Supplemental Fig. S1, *A* and *B*) and glucose homeostasis (Fig. 1). Hereby, we further characterized the model by studying the endocrine function, including insulin and reproductive hormones such as FSH, LH, 17β-estradiol, and testosterone (Table 1). As observed before, the severe impairment in all the parameters related to metabolic homeostasis (HOMA2), significantly improved after diet reversal (Fig. 1). HFD mice had a β-cell function ~3 and twofold higher than those of CTRL and HFD_t (Fig. 1*A*). Influence on glucose sensitivity (%S) (Fig. 1*B*) and insulin resistance (IR) (Fig. 1*C*) was even more pronounced; a 10- and 5-fold increase was observed in HFD animals when compared with CTRL and HFD_t, respectively. Plasma insulin levels were found to be increased in HFD mice, and notably, diet correction restored plasma insulin levels (Table 1).

Dietary correction in adulthood after HFD in early life does not restore the decreased sperm quality. We collected epididymal sperm immediately after euthanization. Sperm motility and concentration were promptly assessed, according to standard protocols. Sperm viability and morphology were evaluated after specific staining techniques and using optical microscopy. We have found no differences in sperm counts between groups (Fig. 2). However, mice fed HFD, even if transiently, displayed reduced sperm motility (CTRL: 81.6 ± 4.6%; HFD: 69.1 ± 7.4%; HFD_t: 65.9 ± 14.5%) and sperm viability (CTRL: 48.2 ± 8.1%; HFD: 38.1 ± 7.2%; HFD_t: 34.4 ± 6.6%). Regarding sperm morphology (Table 2), we used three different classification systems: descriptive (six defects), categorical (three categories) and binomial (normal/abnormal). On the basis of the χ^2 test, we found that sperm morphology distribution is different between groups. Notably, recurring to ANOVA and Tukey's HSD, we

Table 1. *Fasting glycemia and serum concentrations of insulin, FSH, LH, 17β-estradiol, and testosterone in mice fed standard chow (CTRL), life-long high-fat diet (HFD), and those subjected to diet correction after 60 days (HFD_t)*

Analyte	CTRL ($n = 8$)	HFD ($n = 8$)	HFD_t ($n = 8$)
Fasting glucose, mg/dL	94.50 ± 7.94	116.08 ± 15.26***	84.91 ± 9.91####
Insulin, nmol/mL	0.49 ± 0.68	3.56 ± 1.75****	0.67 ± 0.25####
FSH, nmol/mL	6.60 ± 2.83	4.25 ± 3.18	3.77 ± 2.67
LH, nmol/mL	435.99 ± 79.50	406.89 ± 61.62	470.30 ± 28.34
17β-estradiol, pmol/mL	348.89 ± 46.55	335.46 ± 114.04	413.87 ± 108.97
Testosterone, nmol/mL	15.88 ± 0.58	15.88 ± 0.48	15.23 ± 0.97

Fasting glycemia was evaluated using a glucometer (One Touch Ultra Lifescan-Johnson, Milpitas, CA). Hormones were quantified by ELISA assay kits. Results are expressed as means ± SD (units disclosed in the table). CTRL, standard chow; HFD, high-fat diet; HFD_t, transient high-fat diet. Data were tested by one-way ANOVA with the Tukey highly significant difference test for group comparison. Significance was considered when $P < 0.05$. * vs. CTRL. # vs. HFD. ***$P < 0.001$; ****$P < 0.0001$; ####$P < 0.0001$.

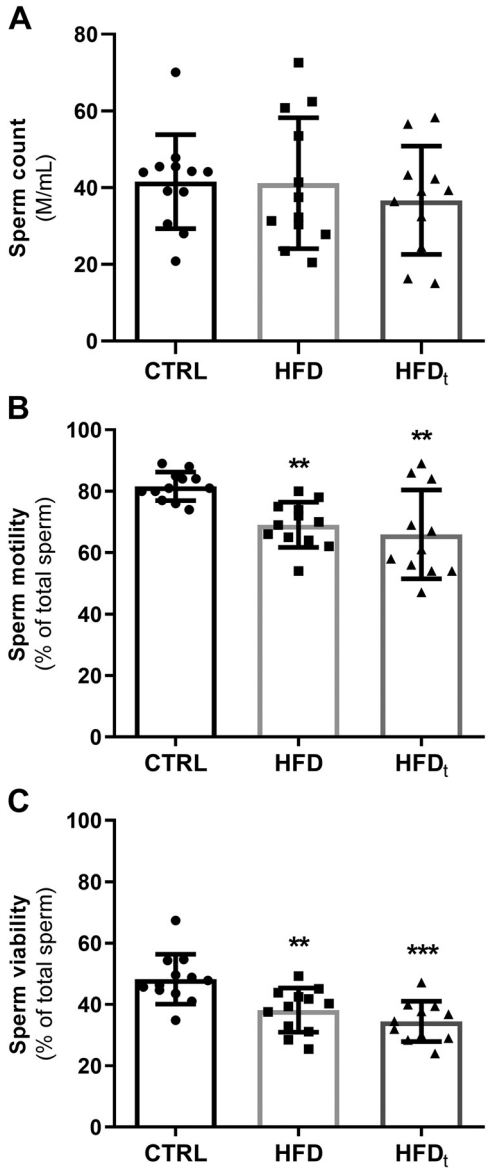

Fig. 2. Epididymal sperm parameters of mice fed standard chow (CTRL) or lifelong high-fat diet (HFD) or subjected to diet correction after 60 days (HFD_t). Results are expressed as means ± SD. Sperm count is expressed as million spermatozoa per milliliter (M/mL), while other parameters are expressed as the percentage of total sperm cells. Individual values are represented (● CTRL denotes standard chow; ■ denotes an HFD, high-fat diet; ▲ denotes HFD_t, transient high-fat diet). Data were tested by one-way ANOVA with the Tukey highly significant difference (HSD) test for group comparison. Significance was considered when $P < 0.05$. $^{**}P < 0.01$; $^{***}P < 0.001$.

have found differences in the prevalence of pinhead, flattened head, bent neck, and overall head defects, especially relative to HFD_t. Despite the observed changes in sperm parameters, diet did not influence reproductive outcomes (Supplemental Table S2). No significant correlations were found between sperm and fertility parameters (data not shown).

Testicular mitochondrial function and bioenergetics are not affected by high-fat diets. Mitochondria were isolated from a whole testis to evaluate relevant parameters related to its activity and physiology. Particularly, relative protein expression of mitochondrial OXPHOS complexes was assessed by Western blot analysis, and the activities of complexes I, II, IV and citrate synthase were evaluated by colorimetric/fluorometric assays (Supplemental Table S3). Testicular bioenergetics were evaluated on the basis of testicular content of adenine nucleotides (ATP, ADP, and AMP), quantified by HPLC (Supplemental Table S4). These nucleotides were extracted from the same testis used to isolate the mitochondria-rich fraction. There were no differences between any of the experimental groups.

A high-fat diet promotes a decrease in the activity of antioxidant defenses in testis. Lipid peroxidation and activity of enzymes of the antioxidant defense system were evaluated in mitochondria-free cytosolic fraction obtained from a whole-testis homogenate. The dietary regime did not influence testicular levels of lipid peroxidation products (Fig. 3*A*). Additionally, activities of the cytosolic GPx and SOD were similar in the testes of the mice from the different groups (Fig. 3, *B* and *C*). Conversely, mitochondria-free cytosolic fraction obtained from the testes of HFD group mice exhibited a decrease in CAT (CTRL: 747.66 ± 141.46 nmol $O_2 \cdot min^{-1} \cdot mg\ protein^{-1}$; HFD: 552.41 ± 91.51 $O_2 \cdot min^{-1} \cdot mg\ protein^{-1}$; HFD_t: 670.02 ± 107.21 $O_2 \cdot min^{-1} \cdot mg\ protein^{-1}$) and GSR activities (CTRL: 133.14 ± 11.31 nmol $NADPH \cdot min^{-1} \cdot mg\ protein^{-1}$; HFD: 114.00 ± 11.53 nmol $NADPH \cdot min^{-1} \cdot mg\ protein^{-1}$; HFD_t: 120.44 ± 9.14 nmol $NADPH \cdot min^{-1} \cdot mg\ protein^{-1}$).

Testicular lipid metabolism is irreversibly affected by an HFD during early life. Metabolites were obtained from a whole testis using a protocol based on chloroform-methanol-water extraction, resulting in a polar and apolar fractions. In the polar fraction, analyzed by ^{1}H-NMR, various phospholipid-related metabolites and lipid precursors were detected (Table 3). HFD had a marked influence on the composition of polar lipids, as observed in the levels of phospholipid head groups like myoinositol, choline, or glycerol, or choline-related glycerophosphocholine (GPC). Reversal from HFD to normal diet tended to normalize metabolite levels.

The apolar fraction of the testicular extract was characterized by GC-MS after transmethylation. The identified fatty acids

Table 2. *Sperm morphology distribution, according to different classifications, in mice fed standard chow, lifelong high-fat diet, and high-fat diet with diet correction after 60 days*

Sperm Morphology	CTRL ($n = 9$)	HFD ($n = 12$)	HFD_t ($n = 9$)	χ^2 test
Normal, %	39.79 ± 6.01	33.82 ± 6.74	36.51 ± 4.08	106.83****
Decapitated, %	12.10 ± 5.27	11.19 ± 3.61	12.18 ± 3.11	
Pinhead, %	3.70 ± 1.30	6.20 ± 1.26**	6.68 ± 1.94**	
Flattened head, %	3.92 ± 0.76	4.62 ± 1.20	6.02 ± 0.86$^{***,\#}$	
Bent neck, %	6.49 ± 0.97	9.38 ± 3.64	5.30 ± 1.97$^{\#\#}$	
Coiled tail, %	34.00 ± 5.73	34.77 ± 7.06	33.32 ± 2.46	
Normal, %	39.79 ± 6.01	33.82 ± 6.74	36.51 ± 4.08	48.57****
Head defects, %	19.72 ± 3.82	22.03 ± 4.52	24.88 ± 2.45*	
Tail defects, %	40.49 ± 5.58	44.15 ± 6.41	38.61 ± 3.00	
Normal, %	39.79 ± 6.01	33.82 ± 6.74	36.51 ± 4.08	26.16****
Abnormal, %	60.21 ± 6.01	66.18 ± 6.74	63.49 ± 4.08	

Results are expressed as mean (% of total sperm cells) ± standard deviation. CTRL – standard chow; HFD – high-fat diet; HFD_t – transient high-fat diet. Sperm count distributions across groups were tested using the χ^2 test. Differences between groups for each morphological classification were tested by one-way ANOVA with Tukey's HSD. For both methods, significance was considered when $P < 0.05$. $\#P < 0.05$vs. HFD. $^{*}P < 0.05$, vs. CTRL; $^{**}P < 0.01$; $^{***}P < 0.001$; $^{****}P < 0.0001$.

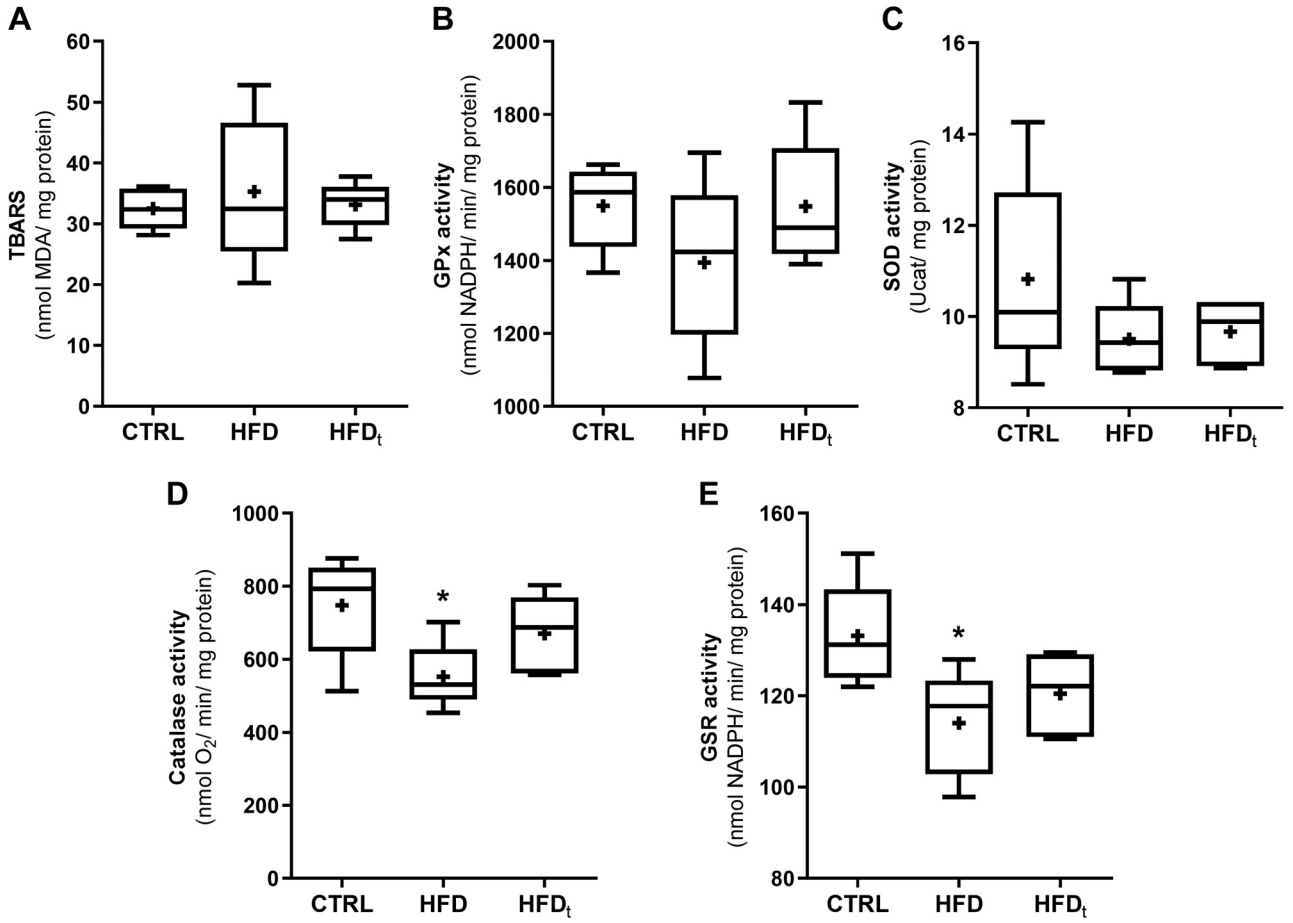

Fig. 3. Lipid peroxidation [thiobarbituric acid reactive species (TBARS) assay] and activity of the four main enzymes of the antioxidative defense metabolism: superoxide dismutase (SOD), glutathione-disulfide reductase (GSR), glutathione peroxidase (GPx) and catalase (CAT) in the testis of mice standard chow (CTRL) or lifelong high-fat diet (HFD) or subjected to diet correction after 60 days (HFD_t). Two outliers were excluded from the analysis resulting in $n = 5$ for every group. Results are expressed as Tukey whisker boxes [median, 25th to 75th percentiles ± 1.5 interquartile range (IQR]. Data were tested by one-way ANOVA with the Tukey highly significant difference test for group comparisons. Significance was considered when $P < 0.05$. +Group average. * vs. CTRL. *$P < 0.05$.

(FAs) were quantified, and their relative abundance is displayed in Supplemental Table S5. Dietary intervention promoted a meta-state between CTRL and HFD conditions for most of the identified FAs (e.g., palmitic acid and stearic acid). The only exception was vaccenic acid (C18:1n-7), which is twice more abundant in testes of HFD_t mice than in CTRL. After grouping FAs by degree of unsaturation and the position of the double bonds (Supplemental Table S5 and Fig. 4), we observed that the most abundant FA family in the testis of CTRL and HFD_t groups are the saturated fatty acids (SFAs) (55.79% and

Table 3. *Polar lipid metabolites detected by ^{1}H-NMR in testicular extracts of mice fed standard chow, lifelong high-fat diet, and those subjected to diet correction after 60 days*

	Metabolite	CTRL ($n = 6$)	HFD ($n = 6$)	HFD_t ($n = 5$)
Lipid Intermediaries	Glycerol	$7.50 \times 10^{-3} \pm 8.48 \times 10^{-4}$	$9.26 \times 10^{-3} \pm 2.58 \times 10^{-4}$**	$7.82 \times 10^{-3} \pm 7.14 \times 10^{-4}$##
	Ethanolamine [a]	$1.75 \times 10^{-3} \pm 2.21 \times 10^{-4}$	$1.74 \times 10^{-3} \pm 1.45 \times 10^{-4}$	$1.48 \times 10^{-3} \pm 1.31 \times 10^{-4}$*, #
	Phosphoethanolamine	$2.01 \times 10^{-2} \pm 1.75 \times 10^{-3}$	$2.01 \times 10^{-2} \pm 5.93 \times 10^{-4}$	$1.99 \times 10^{-2} \pm 9.14 \times 10^{-4}$
	Myoinositol	$4.94 \times 10^{-3} \pm 4.85 \times 10^{-4}$	$5.54 \times 10^{-3} \pm 2.69 \times 10^{-4}$*	$4.58 \times 10^{-3} \pm 3.16 \times 10^{-4}$ ##
	3-Hydroxybutyrate	$6.68 \times 10^{-2} \pm 1.08 \times 10^{-2}$	$5.70 \times 10^{-2} \pm 3.40 \times 10^{-3}$	$5.97 \times 10^{-2} \pm 6.44 \times 10^{-3}$
Choline Metabolism	Choline	$1.32 \times 10^{-2} \pm 1.56 \times 10^{-3}$	$0.98 \times 10^{-2} \pm 1.29 \times 10^{-3}$**	$1.12 \times 10^{-2} \pm 1.32 \times 10^{-3}$
	Phosphocholine	$2.01 \times 10^{-2} \pm 1.75 \times 10^{-3}$	$2.01 \times 10^{-2} \pm 5.93 \times 10^{-4}$	$1.99 \times 10^{-2} \pm 9.14 \times 10^{-4}$
	Glycerophosphocholine	$3.00 \times 10^{-3} \pm 3.39 \times 10^{-4}$	$4.26 \times 10^{-3} \pm 3.70 \times 10^{-4}$****	$3.81 \times 10^{-3} \pm 2.67 \times 10^{-4}$*

Results are expressed as mean (arbitrary units) ± standard deviation. CTRL – standard chow; HFD – high-fat diet; HFD_t – transient high-fat diet. Results were tested by one-way ANOVA with Tukey's HSD, except where stated otherwise. Significance was considered when $P < 0.05$. [a]Kruskal-Wallis test, unadjusted P value. *$P < 0.05$, vs. CTRL; #$P < 0.05$ vs. HFD; **$P < 0.01$; ****$P < 0.0001$; ##$P < 0.01$.

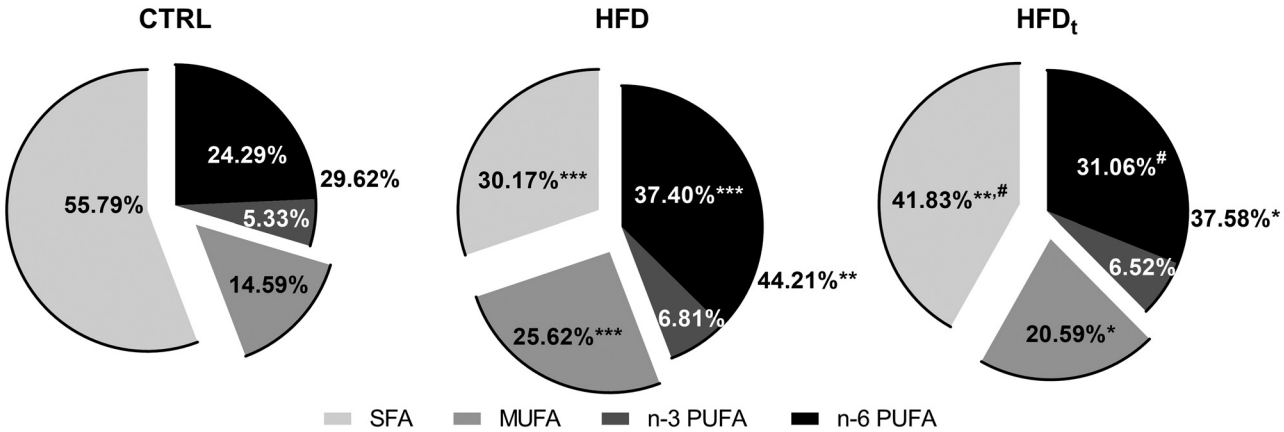

Fig. 4. Relative abundance of lipids in the apolar fraction of testicular extracts of mice fed standard chow (CTRL) or lifelong high-fat diet (HFD) or subjected to diet correction after 60 days (HFD_t), grouped by saturation. CTRL, standard chow; HFD, high-fat diet; HFD_t, transient high-fat diet. The results were tested by one-way ANOVA with the Tukey honestly significant difference test for post hoc group comparisons. Significance was considered when $P < 0.05$. * versus CTRL; # vs. HFD. *$P < 0.05$; **$P < 0.01$; ***$P < 0.001$; #$P < 0.05$. MUFAs, monounsaturated fatty acids; PUFAs, polyunsaturated fatty acids; SFA, saturated fatty acids.

41.83%, respectively), while polyunsaturated fatty acids (PUFAs) are the most abundant in the testis of mice from the HFD group (44.21%). HFD and HFD_t mice also had increased testicular relative abundance of monosaturated fatty acids (MUFAs) (26% and 21%, respectively), with increased accumulation of oleic acid (C18:1n-9). Moreover, Supplemental Table S5 also shows indirect measures for the anti-inflammatory/proinflammatory potential via lipid mediators (C22:6n-3/C20:4n-6 ratio), the combined activity of Δ5- and Δ6-desaturases (D5D and D6D) (C20:4n-6/C18:2n-6 ratio), and the activity of Δ4-desaturases (D4D) (C22:5n-6/C20:4n-6 ratio).

Male reproductive dysfunction caused by HFD is correlated to lipid dysmetabolism in testes. Our main aim was to evaluate whether a dietary intervention in early adulthood can prevent damage to male reproductive health. However, as in previous studies (12, 25), groups were not considered when testing for correlations. Assuming that all mice are equivalent before being fed by a specific diet regimen, our test hypothesis is that some pairs of variables vary proportionally in response of HFD. Those pairs reflect the most relevant (discriminant) variables; therefore, the variables that must be included in the multivariate model. In a correlation matrix (Fig. 5*A*), we tested variables of mitochondrial function, bioenergetics, endocrine function, and antioxidant defenses against sperm parameters. We found a significant negative correlation between Complex I activity and the prevalence of pin head sperm defect ($r = -0.577$; $P = 0.024$). Regarding bioenergetics, the increase in testicular content in ATP ($r = 0.517$; $P = 0.034$) and ATP/ADP ratio ($r = 0.592$; $P = 0.012$) was correlated with elevated sperm counts. AMP ($r = -0.638$; $P = 0.011$) and AMP/ATP ratio ($r = -0.703$; $P = 0.003$) were inversely correlated to sperm head defects, particularly decapitated sperm ($r = -0.627$; $P = 0.012$ and $r = -0.689$; $P = 0.005$). Conversely, testicular energy charge was positively correlated to both parameters ($r = 0.733$; $P = 0.002$ and $r = 0.633$; $P = 0.011$). Concerning endocrine function, most correlations were found in glucose homeostasis. Elevated serum levels of insulin ($r = -0.425$; $P = 0.043$), HOMA2-%B ($r = -0.523$; $P = 0.010$) and HOMA2-IR ($r = -0.438$; $P = 0.037$) were correlated with lower sperm viability. HOMA2-%S behaved contrarily to the former ($r = 0.424$; $P = 0.044$). FSH showed a protective effect against sperm head defects ($r = -0.464$; $P = 0.039$), namely pin ($r = -0.505$; $P = 0.023$) or flattened head ($r = -0.673$; $P = 0.001$) defects. Concerning antioxidant defenses, only SOD activity presented a significant inverse correlation to sperm concentration ($r = -0.527$; $P = 0.030$). Significantly correlated variables were selected for PCA, to evaluate their predictive power (i.e., if samples were clustered according to their diet using these variables as predictors). These correlations promote a significant clustering of samples, according to their experimental group, and there is no overlap between groups, considering 2 PCs (Fig. 5*B*).

In the second correlation matrix (Fig. 6*A*), sperm parameters were correlated against testicular lipid metabolite levels. Testicular content in SFAs and PUFAs had a mirror effect over the prevalence of bent neck and coiled tail sperm defects, while SFAs were negatively correlated with bent sperm neck defects ($r = -0.668$; $P = 0.035$) and positively correlated with coiled sperm tail defects ($r = 0.649$; $P = 0.042$). MUFAs had the opposite relation to bent sperm neck ($r = 0.744$; $P = 0.014$) and to coiled sperm tail ($r = -0.663$; $P = 0.037$). Globally, lipid precursors correlated positively with sperm viability. Testicular glycerol ($r = 0.612$; $P = 0.020$) and myoinositol ($r = 0.592$; $P = 0.026$), however, displayed a positive correlation with the prevalence of bent neck sperm. Choline is positively correlated to normal morphology of sperm ($r = 0.609$; $P = 0.021$), while negatively correlated to tail defects ($r = 0.614$; $P = 0.019$). The two-dimensional projection of the PCs extracted by PCA (Fig. 6*B*) reveals a clear separation of the samples according to their group.

DISCUSSION

Overweight and obesity have reached pandemic proportions worldwide. Simultaneously, the prevalence of childhood obesity is increasing, leading to the onset of obesity-associated comorbidities, such as T2DM, at younger ages. Reproductive function depends on metabolic homeostasis. Several reports link the prevalence of metabolic disease with lower sperm quality (14, 19, 51). In this study, we used a rodent model to investigate whether a dietary intervention to replace an HFD with a balanced diet in early adulthood, is effective in reversing or

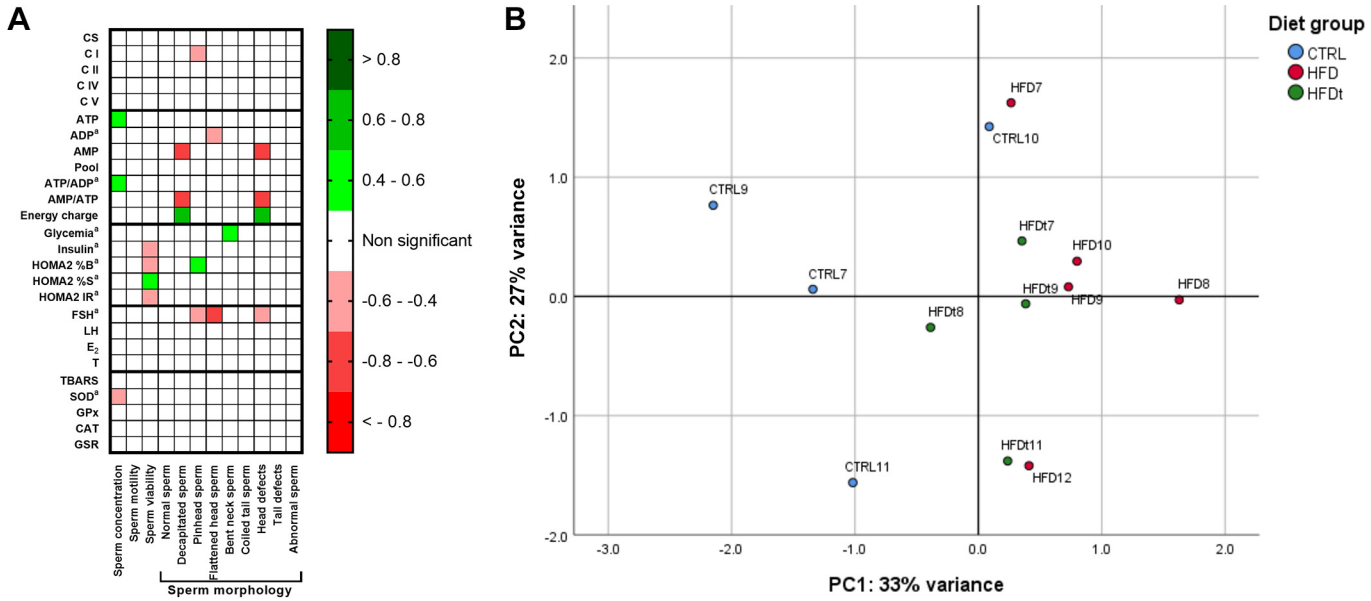

Fig. 5. Correlations between sperm parameters to endocrine, antioxidant, mitochondrial, and bioenergetic parameters. *A*: individual scores for the previously assessed parameters were correlated using the parametric Pearson correlation ($n = 24$). Values are represented as Pearson r coefficients, according to the color scale, when $P < 0.05$. *B*: sample distribution according to 2 principal components extracted by principal components analysis, and on the basis of correlations between sperm parameters to endocrine, antioxidant, mitochondrial, and bioenergetic parameters ($n = 10$). [a]After base-10 logarithmic transformation. CS, citrate synthase; C I, complex I activity; C II, complex II activity; C IV, complex IV activity; C V, complex V activity; Pool, total adenosine nucleotide pool; glycemia, fasting glycemia; FSH, serum follicle-stimulating hormone; LH, serum leutinizing hormone; E_2,serum 17β-estradiol; T, serum testosterone; TBARS, thiobarbituric acid-reactive species assay (lipid peroxidation); SOD, superoxide dismutase activity; GPx, glutathione peroxidase activity; CAT, catalase activity; GSR, glutathione-disulfide reductase activity.

preventing the negative effects of childhood obesity in fat accumulation, metabolic homeostasis, and sperm quality. Particularly, we evaluated whether diet intervention is effective in normalizing testicular metabolic and lipid balance, and sperm quality later in life. Further, we integrated all data of metabolomics and lipidomics to elucidate the importance of lipids in mechanisms involved in the onset and/or recovery of the fertility phenotypes induced by HFD in early life.

We have previously demonstrated that this model induces phenotypic traits related to obesity and metabolic syndrome,

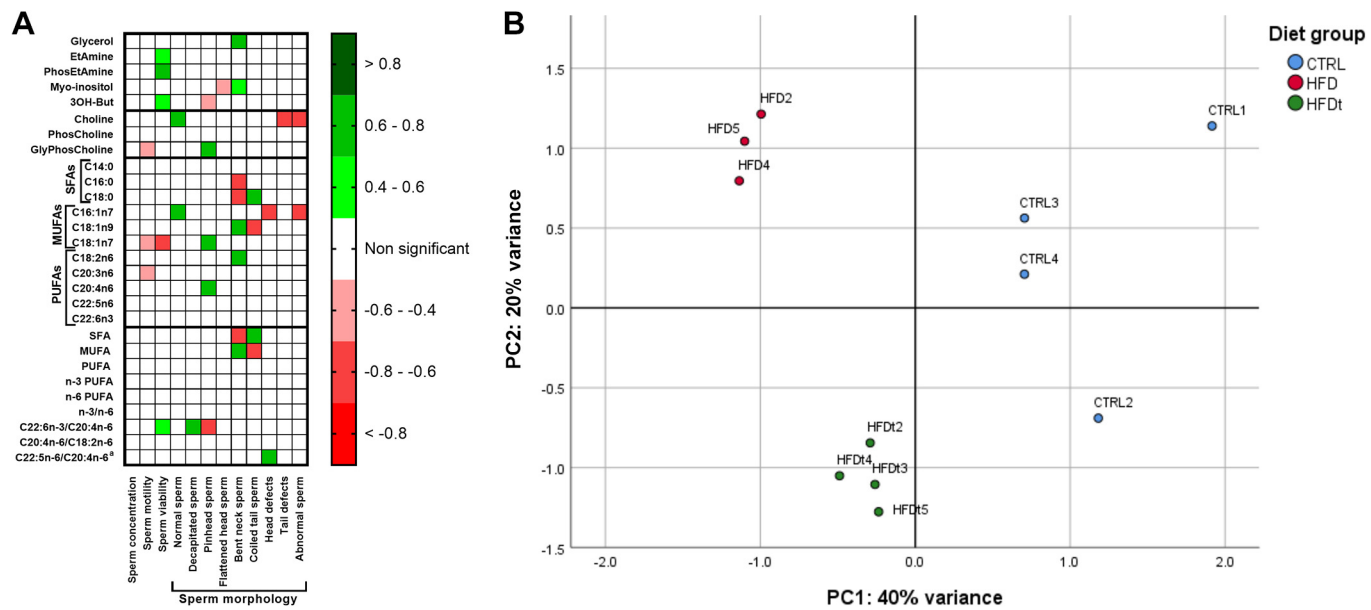

Fig. 6. Correlation of sperm parameters to testicular lipids and lipid precursors. *A*: individual scores for the previously assessed parameters were correlated using the parametric Pearson correlation ($n = 14$). Values are represented as Pearson r coefficients, according to the color scale, when $P < 0.05$. *B*: sample distribution according to 2 principal components (PCs) extracted by principal components analysis, and based on correlations between sperm parameters to testicular lipids and lipid precursors ($n = 11$). [a]Spearman rho coefficients, as the normality assumption was violated for this variable. EtAmine, ethanolamine; PhosEtAmine, phosphoethanolamine; 3OH-But, 3′-hydroxybutyrate; PhosCholine, phosphocholine; GlyPhosCholine, glycerophosphocholine; SFAs, saturated fatty acids; MUFA, monounsaturated fatty acid; PUFA, polyunsaturated fatty acid.

based on biometric and physiological tests for glucose intolerance (ipGTT) and insulin resistance (ipITT) (12). We have shown that HFD promoted fat deposition in white adipose tissue pads and liver, which were positively correlated with poorer performance in ipGTT and ipITT. In this report, we calculated HOMA2 indexes based on fasting glycemia and fasting insulin levels (30). Although HOMA2 application to animal models is often criticized (68), as it has been developed on the basis of a large human database, it has shown an acceptable goodness of fit for mouse and other mammals (4, 5), and has a high correspondence to ipITT, ipGTT, and their respective AUCs (1). As its precursor, HOMA is based upon serum fasting glycemia and insulinemia, therefore providing a better physiological characterization of glucose homeostasis. The methodology for quantifying hormonal serum concentrations at euthanization was ELISA, for all selected hormones. Insulin was the only hormone measured that was found to be altered when comparing hormonal levels in the serum of mice from the different groups. HOMA2 showed that dietary intervention is not capable to completely reverse the effects of an HFD during early life in β-cell function and insulin sensitivity, despite total recovery of insulin resistance index. Despite these results not being novel (12), it is relevant to state the high degree of correspondence with our previous results, obtained using different methods for glucose homeostasis assessment.

Although testosterone aromatization into estradiol has been widely reported in patients with obesity, our results support recent research showing that this effect may be negligible (6, 52). Although another study suggests marked changes in sex hormone levels in HFD rodents (8), circulating levels of fertility-related hormones were not influenced by dietary regimes in this particular study (Table 1). Yet, endocrine function is strongly correlated with sperm quality, especially glucose homeostasis and FSH secretion (3, 11, 55) (Fig. 5*A*). In this context, Sertoli cells (SCs) may be the mediator between both factors and sperm quality. SCs nurse differentiating germ cells during spermatogenesis, and their function is modulated by metabolic (26, 56) and endocrine (34–36, 54) factors, with significant impact on mature spermatozoa (49). Fat deposition in the abdominal area, in humans, is correlated with poor sperm quality (15, 21), likely due to increased testicular temperature (17, 24) and local inflammation (32). In our previous work (12), we also reported reduced sperm quality, which was associated with fat deposition. Moreover, there is a decrease in the activity of antioxidant enzymes (Cat and GSR) in the testes of lifelong HFD-fed mice. Therefore, it is possible that extra lipid intake, notably in PUFAs, is the cornerstone in testicular antioxidant balance. This hypothesis is supported by the differences in lipid fractions between groups (Fig. 4), the differences in the correlations of lipid fractions against sperm parameters (Fig. 6*A*), and the sample separation achieved by the corresponding PCA (Fig. 6*B*). Nonetheless, more studies will be needed to confirm this hypothesis, particularly by using a model in which HFD is replaced by a high-fat, low-PUFA diet. Moreover, we have not considered the potential contamination of testicular lipid profile by serum. Yet, testes were decapsulated before homogenization to hinder this issue. Besides, the interference of serum lipid profile is unlikely considering blood to testis volume (27) and a previous study comparing testicular and serum lipid profiles (44).

HFD is the culprit for testicular lipid dysmetabolism. The proportion of SFAs is the lowest in testes of mice from the HFD group, and the highest in testis from mice of the CTRL group. Contrastingly, MUFA and PUFA fractions were more abundant in HFD than in the CTRL group. As lard, one of the main components of the diet formulations, is rich in oleic acid (18:1n9), it is not surprising that HFD and HFD_t testes are enriched in this fatty acid. Yet, the relative content of MUFAs compared with PUFAs, in both groups, suggests that oleic acid and other MUFAs are unsaturated into PUFAs. Besides, the detected n-3 and n-6 long-chain PUFAs can only be synthesized after their precursors, the linoleic and linolenic acid are obtained by diet, as they cannot be synthesized de novo in mammals (39). According to Koeberle et al. (28), mammals store large amounts of PUFAs in testes during puberty, by the action of the lysophosphatidic acid acyltransferase 3, resulting in a unique FA profile. For instance, docosapentaenoic acid (C22:5n-6, n-6 DPA) is more abundant in the testis than in other mammalian tissues (7, 74). Although several studies describe n-6 DPA-enrichment in various tissues due to HFD (16, 43, 50), testicular content of DPA was unchanged in our model, but we observed testicular enrichment in other n-6 FAs (Supplemental Table S5).

Regarding PUFAs, the n-3/n-6 ratio in testis supports an amelioration in testicular metabolism after ceasing HFD feeding at early adulthood. The Δ6 desaturase (D6D) has been associated with the deleterious effects of HFD, particularly regarding glucose resistance (23). The dietary n-3/n-6 ratio intake, for humans, is ideally close to 1, and lower ratios (n-6 enrichment) are associated with health deterioration, including increased cardiovascular risk (59). In human testis, a lower n-3/n-6 ratio has been reported in oligo and asthenozoospermia (73). Herein, we found a much lower n-3/n-6 ratio (0.22) in testicular FA content, in the CTRL group. Yet, this ratio was significantly lower (0.18) in HFD-fed mice during their lifetime. Considering the critical role of docosahexaenoic acid (C22:6n-3, DHA) in spermatogenesis, the detrimental content of n-3 in testis may be associated with the observed phenotype, as it cannot balance the proinflammatory environment induced by HFD. Effectively, DHA supplementation was shown to improve testicular n-3/n-6 ratio, concomitantly improving antioxidant balance (63). However, in our study, sperm parameters did not correlate to the testicular n-3/n-6 ratio.

Although the HFD formulation had similar relative amounts of SFAs, MUFAs, and PUFAs comparing to the standard chow, the C18:3n-3/C18:2n-6 molar ratio is an order of magnitude higher in HFD (according to the manufacturer information). Interestingly, testicular cells responded to this difference by accumulating even more n-6 PUFAs, without changing their n-3 PUFA content (Fig. 4/Supplemental Table S5). Moreover, n-6 PUFA changes are distinguished not only by an increase in the relative abundance of dietary available linoleic acid (C18:2n-6) but also by an increase of dihomo-γ-linolenic acid (C20:3n-6), and arachidonic acid (C20:4n-6; AA), which are obtained from linoleic acid by an enzyme-catalyzed desaturation-elongation process. This may reflect an overall inhibition of the D4Ds and D5D induced by HFD, notably by the relative enrichment in the dietary n-3. D6D is considered the rate-limiting enzyme in the desaturation-elongation processes in mammalian cells, but according to the relative abundance of n-6 PUFAs to n-3 PUFAs and the C20:4n-6/C18:2n-6 ratio, HFD does not change its activity nor is it overwhelmed by the extra dietary n-3. Therefore, testicular metabolic pathways involving n-6 PUFA

remodeling and metabolism exhibit high sensitivity to the excess of dietary fat (Fig. 4).

The structural importance of phospholipids and its FA composition to cell membrane fluidity should not be overlooked (31). Testicular SFA content is negatively correlated with bent neck defects, while it is positively correlated with coiled tail defects. Interestingly, MUFAs present mirrored correlations. This observation may be linked to the different membrane composition of the midpiece (neck) and the tail, or even to different membrane lipid needs of germ cells at different spermatogenic stages (70). However, because of the limited availability of testicular samples, it was not possible to estimate the detailed testicular content of neutral lipid and phospholipid classes, besides the total lipid profile. In this context, it is noteworthy that FAs from the same lipid saturation family can result in opposite outcomes in testicular function. DHA is reduced in testes of acyl-CoA synthetase isoform 6 (ACSL6) knockout (KO) mice, leading to an enrichment in the AA (20). This change fosters a proinflammatory environment, as AA is an n-6 PUFA and precursor of proinflammatory eicosanoids, whereas DHA is an n-3 PUFA and precursor of resolvins. According to those authors, ACSL6-KO mice suffered from subfertility, with hypogonadism, oligozoospermia, reduced number of germ cells, and morphological abnormalities of the seminiferous epithelium. Our data show that HFD group presented overlapping phenotypes, such as AA accumulation in testes and poorer sperm parameters, although without DHA depletion in testes, likely due to its dietary intake. Particularly, testicular AA content is positively correlated to sperm pin head defects. However, Hale et al. (20) further reported that DHA-rich and AA-rich phospholipids are delocalized in testes of ACSL6-KO mice. So, the relative testicular content in those FAs is crucial to maintain a normal testicular ultrastructure and spermatogenesis, although some caution must be taken, as the characterization of FAs was not quantitative. Despite the different proportions in lipid fractions between diet regimens, it is not possible to state whether absolute testicular FA content is enriched after HFD.

HFD promotes a positive feedback toward a proinflammatory state in testis. Both n-3/n-6 and C22:6n-3/C20:4n-6 reflect a shift toward proinflammatory pathways in the testis of mice continuously fed by HFD (Supplemental Table S5). Interestingly, the same group presented lower CAT and GSR activity and lower potential to prevent oxidative damage. The testicular enrichment in C18:1n-9, in HFD mice, may promote cell membrane fluidity in testicular cells and, consequently, their vulnerability to peroxidation and phospholipase A2. Ultimately, it leads to increased release of PUFAs, particularly AA, a central precursor of pro-inflammatory pathways (leukotrienes, thromboxanes and prostaglandins). Overall, the present data indicate that HFD shifts the cellular redox environment toward a more prooxidant and pro-inflammatory state, enhancing testes susceptibility for oxidative stress and inflammatory processes development. Thus, the absence of changes in lipid peroxidation (TBARS) and in the activity of mitochondrial Electron-Transfer Chain activity complexes suggest that HFD by itself seems not to be enough stimulus to trigger oxidative stress. It was reported that HFD causes an increase in antioxidant metabolites in testis, notably GSH and betaine (12). Although we cannot rule out that the decreased activity of Cat and GSR can emerge from post-translational changes (e.g., acetylation, phosphorylation and ubiquitination), it was reported that HFD has not only a negative impact (decrease) on the expression of testicular antioxidant enzymes (18, 32), but also promotes an increase in antioxidant metabolites in testes, notably GSH and betaine (12). Thus, the increased testicular GSH and betaine levels may be enough to keep the redox balance in testis despite the decreased enzymatic antioxidant protection.

In addition to this, lipolysis can be another contributor to the observed differences in lipid fractions, and a critical process to mediate membrane integrity and fluidity of all cells in testicular tissue. It is well known that dietary MUFAs promote lipolysis (48). Changes in testicular glycerol, choline, myo-inositol and glycerophosphocholine in HFD (and partially in HFD_t) are likely due to lipolysis and indicate increased phospholipid turnover and/or degradation. Nevertheless, lipolysis raises another threat to seminiferous tubules stability. Glycerol accumulates in the testes of HFD and HFD_t mice. Glycerol destabilizes tight junctions and desmosomes between SCs, causing a leaky blood-testis barrier (10). We also observed an accumulation of the organic osmolytes glycerophosphocholine and myoinositol in testes, after HFD. Previously, we reported an accumulation of betaine, glutamine, and glutamate in the same condition (12). Interestingly, this phenomenon has been previously reported in kidney medullar cells, as a response against hypertonic stress (45). FA oxidation requires a hydration step; therefore, the extra dietary intake of FAs can induce hypertonic stress in testes, triggering this response in testicular cells, notably SCs. Our data also suggest a protective effect of choline against sperm tail defects. A recent study linked choline (and betaine) supplementation with lipolysis activation, due to elevated succinate concentration (60) in plasma. Interestingly, we have obtained opposite results in testes, after dietary intervention (12). Yet, our data support a promotion of lipolysis in testes by HFD in early adult life. Again, SCs are likely involved in this outcome, as their metabolic activity has been described to be remodeled toward lipolysis as a response to a high-energy environment, as it is the case of obesity (56). In our model, we have observed that AMP and AMP/ATP ratio inversely correlated with sperm head defects suggesting that energy-consuming pathways can be beneficial to spermatozoa. Conversely, increased testicular energy charge promoted sperm head defects. Additionally, sperm motility was reduced in groups where our data suggest lipolysis overactivation (HFD and HFD_t groups), as supported by the changes observed in metabolites related to phospholipids. An exaggerated accumulation of lipid droplets in the testis leads to lower sperm motility, but a proper FA acid supply is needed for sperm capacitation in the epididymis (37). Thus, different metabolic pathways related to different lipid classes have different roles and importance not only in different testicular cells, but also in different parts of the spermatozoon (66).

In summary, our data demonstrate that an HFD during early life (akin to childhood and puberty) causes an excessive accumulation of unsaturated FAs is testes. A diet intervention, replacing HFD for a balanced diet was proven effective in protecting/preventing metabolic dysfunction. However, an HFD during early life caused irreversible metabolic remodeling in testes, with long-term sperm defects. Dietary intervention in early adulthood promotes lipolysis in testes, particularly from unsaturated FAs, toward the CTRL state, but this process is apparently too slow to recover normal sperm parameters. Mechanistically, our data suggest that HFD promotes a proinflammatory state in testis, aggravated by a positive feedback

system that favors the accumulation of n-6 PUFAs, precursors of inflammatory response signaling molecules. Our model did not allow us to verify whether testicular lipid composition and normal sperm quality could be achieved later in life, but we must also consider that sperm quality declines with age, even in rodents (25). Epigenetic modifications are likely involved in the observed phenotypes after HFD, especially those which have not been reversed by diet switch. Indeed, the prepubertal period is critical for epigenetic remodeling of germ cells (47, 58), and we plan to investigate the influence of those mechanisms in our model in future work. Our findings highlight the importance of preventing childhood obesity, to avoid irreversible damage for the reproductive health of the fathers of tomorrow, with unpredicted effects on their progeny.

ACKNOWLEDGMENTS

We acknowledge the Portuguese Nuclear Magnetic Resonance Network (REDE/1517/RMN/2005) for access to the facilities. We thank Prof. Pedro N. Oliveira (Institute for Biomedical Sciences Abel Salazar - University of Porto, Portugal) for advice on the statistical methods.

GRANTS

This work was supported by the Portuguese Foundation for Science and Technology to L. Crisóstomo (SFRH/BD/128584/2017), M. G. Alves (IFCT2015 and PTDC/MEC-AND/28691/2017), P. F. Oliveira (IFCT2015), UMIB (UID/Multi/00215/2019) and QOPNA (UID/QUI/00062/2019) cofunded by FEDER funds (POCI/COMPETE 2020); by the Portuguese Society of Diabetology to L. Crisóstomo and M. G. Alves ("Nuno Castel-Branco" research grant and Group of Fundamental and Translational Research); by the European Foundation for the Study of of Diabetes to L. Crisóstomo (EFSD Albert Renold travel grant); and by the Croatian Science Foundation to K. Starčević (IP-2016-06-3163).

DISCLOSURES

No conflicts of interest, financial or otherwise, are declared by the authors.

AUTHOR CONTRIBUTIONS

M.G.A., J.F.R., R.L.B., and P.F.O. conceived and designed research; L.C., M.G.A., R.A.V., I.J., K.S., T.M., and L.R. performed experiments; L.C., M.G.A., R.A.V., and P.F.O. analyzed data; L.C., M.G.A., R.A.V., I.J., K.S., T.M., R.L.B., and P.F.O. interpreted results of experiments; L.C. prepared figures; L.C., M.G.A., and P.F.O. drafted manuscript; L.C., M.G.A., R.A.V., I.J., K.S., T.M., J.F.R., R.L.B., and P.F.O. edited and revised manuscript; L.C., M.G.A., R.A.V., I.J., K.S., T.M., L.R., J.F.R., R.L.B., and P.F.O. approved final version of manuscript.

REFERENCES

1. **Allison DB**, **Paultre F**, **Maggio C**, **Mezzitis N**, **Pi-Sunyer FX.** The use of areas under curves in diabetes research. *Diabetes Care* 18: 245–250, 1995. doi:10.2337/diacare.18.2.245.
2. **Alves MG**, **Oliveira PJ**, **Carvalho RA.** Substrate selection in hearts subjected to ischemia/reperfusion: role of cardioplegic solutions and gender. *NMR Biomed* 24: 1029–1037, 2011. doi:10.1002/nbm.1640.
3. **Alves MG**, **Rato L**, **Carvalho RA**, **Moreira PI**, **Socorro S**, **Oliveira PF.** Hormonal control of Sertoli cell metabolism regulates spermatogenesis. *Cell Mol Life Sci* 70: 777–793, 2013. doi:10.1007/s00018-012-1079-1.
4. **Antunes LC**, **Elkfury JL**, **Jornada MN**, **Foletto KC**, **Bertoluci MC.** Validation of HOMA-IR in a model of insulin-resistance induced by a high-fat diet in Wistar rats. *Arch Endocrinol Metab* 60: 138–142, 2016. doi:10.1590/2359-3997000000169.
5. **Avtanski D**, **Pavlov VA**, **Tracey KJ**, **Poretsky L.** Characterization of inflammation and insulin resistance in high-fat diet-induced male C57BL/6J mouse model of obesity. *Animal Model Exp Med* 2: 252–258, 2019. doi:10.1002/ame2.12084.
6. **Bekaert M**, **Van Nieuwenhove Y**, **Calders P**, **Cuvelier CA**, **Batens A-H**, **Kaufman J-M**, **Ouwens DM**, **Ruige JB.** Determinants of testosterone levels in human male obesity. *Endocrine* 50: 202–211, 2015. doi:10.1007/s12020-015-0563-4.
7. **Bieri JG**, **Prival EL.** Lipid composition of testes from various species. *Comp Biochem Physiol* 15: 275–282, 1965. doi:10.1016/0010-406X(65)90131-3.
8. **Borges BC**, **Garcia-Galiano D**, **da Silveira Cruz-Machado S**, **Han X**, **Gavrilina GB**, **Saunders TL**, **Auchus RJ**, **Hammoud SS**, **Smith GD**, **Elias CF.** Obesity-induced infertility in male mice is associated with disruption of Crisp4 expression and sperm fertilization capacity. *Endocrinology* 158: 2930–2943, 2017. doi:10.1210/en.2017-00295.
9. **Caumo A**, **Perseghin G**, **Brunani A**, **Luzi L.** New insights on the simultaneous assessment of insulin sensitivity and β-cell function with the HOMA2 method. *Diabetes Care* 29: 2733–2734, 2006. doi:10.2337/dc06-0070.
10. **Crisóstomo L**, **Alves MG**, **Calamita G**, **Sousa M**, **Oliveira PF.** Glycerol and testicular activity: the good, the bad and the ugly. *Mol Hum Reprod* 23: 725–737, 2017. doi:10.1093/molehr/gax049.
11. **Crisóstomo L**, **Alves MG**, **Gorga A**, **Sousa M**, **Riera MF**, **Galardo MN**, **Meroni SB**, **Oliveira PF.** Molecular mechanisms and signalling pathways involved in the nutritional support of spermatogenesis by Sertoli cells. In: *Sertoli Cells: Methods and Protocols*, edited by Alves MG, Oliveira PF. New York: Humana Press, 2018, p. 129–155.
12. **Crisóstomo L**, **Rato L**, **Jarak I**, **Silva BM**, **Raposo JF**, **Batterham RL**, **Oliveira PF**, **Alves MG.** A switch from high-fat to normal diet does not restore sperm quality but prevents metabolic syndrome. *Reproduction* 158: 377–387, 2019. doi:10.1530/REP-19-0259.
13. **Del Río LA**, **Ortega MG**, **López AL**, **Gorgé JL.** A more sensitive modification of the catalase assay with the Clark oxygen electrode. Application to the kinetic study of the pea leaf enzyme. *Anal Biochem* 80: 409–415, 1977. doi:10.1016/0003-2697(77)90662-5.
14. **Eisenberg ML**, **Sundaram R**, **Maisog J**, **Buck Louis GM.** Diabetes, medical comorbidities and couple fecundity. *Hum Reprod* 31: 2369–2376, 2016. doi:10.1093/humrep/dew200.
15. **Faure C**, **Dupont C**, **Baraibar MA**, **Ladouce R**, **Cedrin-Durnerin I**, **Wolf JP**, **Lévy R.** In subfertile couple, abdominal fat loss in men is associated with improvement of sperm quality and pregnancy: a case-series. *PLoS One* 9: e86300, 2014. doi:10.1371/journal.pone.0086300.
16. **Garg ML**, **Sebokova E**, **Thomson ABR**, **Clandinin MT.** Δ6-desaturase activity in liver microsomes of rats fed diets enriched with cholesterol and/or ω3 fatty acids. *Biochem J* 249: 351–356, 1988. doi:10.1042/bj2490351.
17. **Garolla A**, **Torino M**, **Miola P**, **Caretta N**, **Pizzol D**, **Menegazzo M**, **Bertoldo A**, **Foresta C.** Twenty-four-hour monitoring of scrotal temperature in obese men and men with a varicocele as a mirror of spermatogenic function. *Hum Reprod* 30: 1006–1013, 2015. doi:10.1093/humrep/dev057.
18. **Ghosh S**, **Mukherjee S.** Testicular germ cell apoptosis and sperm defects in mice upon long-term high fat diet feeding. *J Cell Physiol* 233: 6896–6909, 2018. doi:10.1002/jcp.26581.
19. **Guo D**, **Wu W**, **Tang Q**, **Qiao S**, **Chen Y**, **Chen M**, **Teng M**, **Lu C**, **Ding H**, **Xia Y**, **Hu L**, **Chen D**, **Sha J**, **Wang X.** The impact of BMI on sperm parameters and the metabolite changes of seminal plasma concomitantly. *Oncotarget* 8: 48619–48634, 2017. doi:10.18632/oncotarget.14950.
20. **Hale BJ**, **Fernandez RF**, **Kim SQ**, **Diaz VD**, **Jackson SN**, **Liu L**, **Brenna JT**, **Hermann BP**, **Geyer CB**, **Ellis JM.** Acyl-CoA synthetase 6 enriches seminiferous tubules with the omega-3 fatty acid DHA and is required for male fertility in the mouse. *J Biol Chem* 234: 14394–14405, 2019. doi:10.1074/jbc.RA119.009972.
21. **Hammoud AO**, **Gibson M**, **Peterson CM**, **Meikle AW**, **Carrell DT.** Impact of male obesity on infertility: a critical review of the current literature. *Fertil Steril* 90: 897–904, 2008. doi:10.1016/j.fertnstert.2008.08.026.
22. **Hruby A**, **Manson JE**, **Qi L**, **Malik VS**, **Rimm EB**, **Sun Q**, **Willett WC**, **Hu FB.** Determinants and consequences of obesity. *Am J Public Health* 106: 1656–1662, 2016. doi:10.2105/AJPH.2016.303326.
23. **Hucik B**, **Sarr O**, **Nakamura MT**, **Dyck DJ**, **Mutch DM.** Reduced delta-6 desaturase activity partially protects against high-fat diet-induced impairment in whole-body glucose tolerance. *J Nutr Biochem* 67: 173–181, 2019. doi:10.1016/j.jnutbio.2019.02.005.
24. **Ivell R.** Lifestyle impact and the biology of the human scrotum. *Reprod Biol Endocrinol* 5: 15, 2007. doi:10.1186/1477-7827-5-15.
25. **Jarak I**, **Almeida S**, **Carvalho RA**, **Sousa M**, **Barros A**, **Alves MG**, **Oliveira PF.** Senescence and declining reproductive potential: Insight into molecular mechanisms through testicular metabolomics. *Biochim Biophys Acta Mol Basis Dis* 1864: 3388–3396, 2018. doi:10.1016/j.bbadis.2018.07.028.

26. **Jesus TT**, **Oliveira PF**, **Silva J**, **Barros A**, **Ferreira R**, **Sousa M**, **Cheng CY**, **Silva BM**, **Alves MG.** Mammalian target of rapamycin controls glucose consumption and redox balance in human Sertoli cells. *Fertil Steril* 105: 825–833.e3, 2016. doi:10.1016/j.fertnstert.2015.11.032.
27. **Kaliss N**, **Pressman D.** Plasma and blood volumes of mouse organs, as determined with radioactive iodoproteins. *Proc Soc Exp Biol Med* 75: 16–20, 1950. doi:10.3181/00379727-75-18083.
28. **Koeberle A**, **Shindou H**, **Harayama T**, **Yuki K**, **Shimizu T.** Polyunsaturated fatty acids are incorporated into maturating male mouse germ cells by lysophosphatidic acid acyltransferase 3. *FASEB J* 26: 169–180, 2012. doi:10.1096/fj.11-184879.
29. **Kvist U**, **Björndahl L**; **Nordic Association for Andrology, European Society of Human Reproduction and Embryology, Andrology Special Interest Group.** In: *Manual on Basic Semen Analysis: 2002*. Oxford, UK: University Press, 2002.
30. **Levy JC**, **Matthews DR**, **Hermans MP.** Correct homeostasis model assessment (HOMA) evaluation uses the computer program. *Diabetes Care* 21: 2191–2192, 1998. doi:10.2337/diacare.21.12.2191.
31. **Lingwood D**, **Simons K.** Lipid rafts as a membrane-organizing principle. *Science* 327: 46–50, 2010. doi:10.1126/science.1174621.
32. **Liu G-L**, **Zhang Y-M**, **Dai D-Z**, **Ding M-J**, **Cong XD**, **Dai Y.** Male hypogonadism induced by high fat diet and low dose streptozotocin is mediated by activated endoplasmic reticulum stress and IκBβ and attenuated by argirein and valsartan. *Eur J Pharmacol* 713: 78–88, 2013. doi:10.1016/j.ejphar.2013.04.030.
33. **Llewellyn A**, **Simmonds M**, **Owen CG**, **Woolacott N.** Childhood obesity as a predictor of morbidity in adulthood: a systematic review and meta-analysis. *Obes Rev* 17: 56–67, 2016. doi:10.1111/obr.12316.
34. **Martins AD**, **Monteiro MP**, **Silva BM**, **Barros A**, **Sousa M**, **Carvalho RA**, **Oliveira PF**, **Alves MG.** Metabolic dynamics of human Sertoli cells are differentially modulated by physiological and pharmacological concentrations of GLP-1. *Toxicol Appl Pharmacol* 362: 1–8, 2019. doi:10.1016/j.taap.2018.10.009.
35. **Martins AD**, **Moreira AC**, **Sá R**, **Monteiro MP**, **Sousa M**, **Carvalho RA**, **Silva BM**, **Oliveira PF**, **Alves MG.** Leptin modulates human Sertoli cells acetate production and glycolytic profile: a novel mechanism of obesity-induced male infertility? *Biochim Biophys Acta* 1852: 1824–1832, 2015. doi:10.1016/j.bbadis.2015.06.005.
36. **Martins AD**, **Sá R**, **Monteiro MP**, **Barros A**, **Sousa M**, **Carvalho RA**, **Silva BM**, **Oliveira PF**, **Alves MG.** Ghrelin acts as energy status sensor of male reproduction by modulating Sertoli cells glycolytic metabolism and mitochondrial bioenergetics. *Mol Cell Endocrinol* 434: 199–209, 2016. doi:10.1016/j.mce.2016.07.008.
37. **Masaki H**, **Kim N**, **Nakamura H**, **Kumasawa K**, **Kamata E**, **Hirano KI**, **Kimura T.** Long-chain fatty acid triglyceride (TG) metabolism disorder impairs male fertility: a study using adipose triglyceride lipase deficient mice. *Mol Hum Reprod* 23: 452–460, 2017. doi:10.1093/molehr/gax031.
38. **Mendes D**, **Oliveira MM**, **Moreira PI**, **Coutinho J**, **Nunes FM**, **Pereira DM**, **Valentão P**, **Andrade PB**, **Videira RA.** Beneficial effects of white wine polyphenols-enriched diet on Alzheimer's disease-like pathology. *J Nutr Biochem* 55: 165–177, 2018. doi:10.1016/j.jnutbio.2018.02.001.
39. **Miyazaki M**, **Ntambi JM.** Fatty acid desaturation and chain elongation in mammals. In: *Biochemistry of Lipids, Lipoproteins and Membranes* (5th ed.), edited by Vance DE, Vance JE**.** San Diego, CA: Elsevier, 2008, p. 191–211.
40. **Monteiro-Cardoso VF**, **Oliveira MM**, **Melo T**, **Domingues MR**, **Moreira PI**, **Ferreiro E**, **Peixoto F**, **Videira RA.** Cardiolipin profile changes are associated to the early synaptic mitochondrial dysfunction in Alzheimer's disease. *J Alzheimers Dis* 43: 1375–1392, 2015. doi:10.3233/JAD-141002.
41. **Muecke L**, **Simons-Morton B**, **Huang IW**, **Parcel G.** Is childhood obesity associated with high-fat foods and low physical activity? *J Sch Health* 62: 19–23, 1992. doi:10.1111/j.1746-1561.1992.tb01213.x.
42. **Mulholland J**, **Mallidis C**, **Agbaje I**, **McClure N.** Male diabetes mellitus and assisted reproduction treatment outcome. *Reprod Biomed Online* 22: 215–219, 2011. doi:10.1016/j.rbmo.2010.10.005.
43. **Naoe S**, **Tsugawa H**, **Takahashi M**, **Ikeda K**, **Arita M.** Characterization of lipid profiles after dietary intake of polyunsaturated fatty acids using integrated untargeted and targeted lipidomics. *Metabolites* 9: 241, 2019. doi:10.3390/metabo9100241.
44. **Napoli JL**, **McCormick AM.** Tissue dependence of retinoic acid metabolism in vivo. *Biochim Biophys Acta* 666: 165–175, 1981. doi:10.1016/0005-2760(81)90102-8.
45. **Neuhofer W**, **Beck F-X.** Response of renal medullary cells to osmotic stress. In: *Cellular Stress Responses in Renal Diseases*, edited by Razzaque MS, Taguchi T**.** Basel, Switzerland: Karger Publishers, 2005, p. 21–34.
46. **Neves D**, **Valentão P**, **Bernardo J**, **Oliveira MC**, **Ferreira JMG**, **Pereira DM**, **Andrade PB**, **Videira RA.** A new insight on elderberry anthocyanins bioactivity: Modulation of mitochondrial redox chain functionality and cell redox state. *J Funct Foods* 56: 145–155, 2019. doi:10.1016/j.jff.2019.03.019.
47. **Nilsson EE**, **Sadler-Riggleman I**, **Skinner MK.** Environmentally induced epigenetic transgenerational inheritance of disease. *Environ Epigenet* 4: dvy016, 2018. doi:10.1093/eep/dvy016.
48. **O'Connor S**, **Rudkowska I.** Dietary Fatty Acids and the Metabolic Syndrome: A Personalized Nutrition Approach. In: *Advances in Food and Nutrition Research*, edited by Toldrá F**.** Oxford, UK: Academic Press, 2019, p. 43–146.
49. **Oliveira PF**, **Sousa M**, **Silva BM**, **Monteiro MP**, **Alves MG.** Obesity, energy balance and spermatogenesis. *Reproduction* 153: R173–R185, 2017. doi:10.1530/REP-17-0018.
50. **Ostermann AI**, **Waindok P**, **Schmidt MJ**, **Chiu C-Y**, **Smyl C**, **Rohwer N**, **Weylandt K-H**, **Schebb NH.** Modulation of the endogenous omega-3 fatty acid and oxylipin profile in vivo-A comparison of the fat-1 transgenic mouse with C57BL/6 wildtype mice on an omega-3 fatty acid enriched diet. *PLoS One* 12: e0184470, 2017. doi:10.1371/journal.pone.0184470.
51. **Palmer NO**, **Bakos HW**, **Fullston T**, **Lane M.** Impact of obesity on male fertility, sperm function and molecular composition. *Spermatogenesis* 2: 253–263, 2012. doi:10.4161/spmg.21362.
52. **Rastrelli G**, **O'Neill TW**, **Ahern T**, **Bártfai G**, **Casanueva FF**, **Forti G**, **Keevil B**, **Giwercman A**, **Han TS**, **Slowikowska-Hilczer J**, **Lean MEJ**, **Pendleton N**, **Punab M**, **Antonio L**, **Tournoy J**, **Vanderschueren D**, **Maggi M**, **Huhtaniemi IT**, **Wu FCW**; **EMAS study group.** Symptomatic androgen deficiency develops only when both total and free testosterone decline in obese men who may have incident biochemical secondary hypogonadism: Prospective results from the EMAS. *Clin Endocrinol (Oxf)* 89: 459–469, 2018. doi:10.1111/cen.13756.
53. **Rato L**, **Alves MG**, **Dias TR**, **Lopes G**, **Cavaco JE**, **Socorro S**, **Oliveira PF.** High-energy diets may induce a pre-diabetic state altering testicular glycolytic metabolic profile and male reproductive parameters. *Andrology* 1: 495–504, 2013. doi:10.1111/j.2047-2927.2013.00071.x.
54. **Rato L**, **Alves MG**, **Duarte AI**, **Santos MS**, **Moreira PI**, **Cavaco JE**, **Oliveira PF.** Testosterone deficiency induced by progressive stages of diabetes mellitus impairs glucose metabolism and favors glycogenesis in mature rat Sertoli cells. *Int J Biochem Cell Biol* 66: 1–10, 2015. doi:10.1016/j.biocel.2015.07.001.
55. **Rato L**, **Alves MG**, **Socorro S**, **Duarte AI**, **Cavaco JE**, **Oliveira PF.** Metabolic regulation is important for spermatogenesis. *Nat Rev Urol* 9: 330–338, 2012. doi:10.1038/nrurol.2012.77.
56. **Rato L**, **Duarte AI**, **Tomás GD**, **Santos MS**, **Moreira PI**, **Socorro S**, **Cavaco JE**, **Alves MG**, **Oliveira PF.** Pre-diabetes alters testicular PGC1-α/SIRT3 axis modulating mitochondrial bioenergetics and oxidative stress. *Biochim Biophys Acta* 1837: 335–344, 2014. doi:10.1016/j.bbabio.2013.12.008.
57. **Roqueta-Rivera M**, **Stroud CK**, **Haschek WM**, **Akare SJ**, **Segre M**, **Brush RS**, **Agbaga M-P**, **Anderson RE**, **Hess RA**, **Nakamura MT.** Docosahexaenoic acid supplementation fully restores fertility and spermatogenesis in male delta-6 desaturase-null mice. *J Lipid Res* 51: 360–367, 2010. doi:10.1194/jlr.M001180.
58. **Schagdarsurengin U**, **Steger K.** Epigenetics in male reproduction: effect of paternal diet on sperm quality and offspring health. *Nat Rev Urol* 13: 584–595, 2016. doi:10.1038/nrurol.2016.157.
59. **Simopoulos AP.** The importance of the ratio of omega-6/omega-3 essential fatty acids. *Biomed Pharmacother* 56: 365–379, 2002. doi:10.1016/S0753-3322(02)00253-6.
60. **Sivanesan S**, **Taylor A**, **Zhang J**, **Bakovic M.** Betaine and choline improve lipid homeostasis in obesity by participation in mitochondrial oxidative demethylation. *Front Nutr* 5: 61, 2018. doi:10.3389/fnut.2018.00061.
61. **Smith PK**, **Krohn RI**, **Hermanson GT**, **Mallia AK**, **Gartner FH**, **Provenzano MD**, **Fujimoto EK**, **Goeke NM**, **Olson BJ**, **Klenk DC.** Measurement of protein using bicinchoninic acid. *Anal Biochem* 150: 76–85, 1985. doi:10.1016/0003-2697(85)90442-7.
62. **Stanford KI**, **Rasmussen M**, **Baer LA**, **Lehnig AC**, **Rowland LA**, **White JD**, **So K**, **De Sousa-Coelho AL**, **Hirshman MF**, **Patti M-E**, **Rando OJ**, **Goodyear LJ.** Paternal exercise improves glucose metabolism in adult offspring. *Diabetes* 67: 2530–2540, 2018. doi:10.2337/db18-0667.
63. **Starcčević K**, **Maurić M**, **Galan A**, **Gudan Kurilj A**, **Mašek T.** Effects of different n6/n3 ratios and supplementation with DHA and EPA on the

testicular histology and lipogenesis in streptozotocin-treated rats. *Andrologia* 50: e13067, 2018. doi:10.1111/and.13067.

64. **Stokes VJ**, **Anderson RA**, **George JT.** How does obesity affect fertility in men - and what are the treatment options? *Clin Endocrinol (Oxf)* 82: 633–638, 2015. doi:10.1111/cen.12591.
65. **Sumner LW**, **Amberg A**, **Barrett D**, **Beale MH**, **Beger R**, **Daykin CA**, **Fan TWM**, **Fiehn O**, **Goodacre R**, **Griffin JL**, **Hankemeier T**, **Hardy N**, **Harnly J**, **Higashi R**, **Kopka J**, **Lane AN**, **Lindon JC**, **Marriott P**, **Nicholls AW**, **Reily MD**, **Thaden JJ**, **Viant MR.** Proposed minimum reporting standards for chemical analysis Chemical Analysis Working Group (CAWG) Metabolomics Standards Initiative (MSI). *Metabolomics* 3: 211–221, 2007. doi:10.1007/s11306-007-0082-2.
66. **Takei GL**, **Miyashiro D**, **Mukai C**, **Okuno M.** Glycolysis plays an important role in energy transfer from the base to the distal end of the flagellum in mouse sperm. *J Exp Biol* 217: 1876–1886, 2014. doi:10.1242/jeb.090985.
67. **Taylor R.** Interpretation of the correlation coefficient: a basic review. *J Diagn Med Sonogr* 6: 35–39, 1990. doi:10.1177/875647939000600106.
68. **Wallace TM**, **Levy JC**, **Matthews DR.** Use and abuse of HOMA modeling. *Diabetes Care* 27: 1487–1495, 2004. doi:10.2337/diacare.27.6.1487.
69. **Wishart DS**, **Tzur D**, **Knox C**, **Eisner R**, **Guo AC**, **Young N**, **Cheng D**, **Jewell K**, **Arndt D**, **Sawhney S**, **Fung C**, **Nikolai L**, **Lewis M**, **Coutouly MA**, **Forsythe I**, **Tang P**, **Shrivastava S**, **Jeroncic K**, **Stothard P**, **Amegbey G**, **Block D**, **Hau DD**, **Wagner J**, **Miniaci J**, **Clements M**, **Gebremedhin M**, **Guo N**, **Zhang Y**, **Duggan GE**, **Macinnis GD**, **Weljie AM**, **Dowlatabadi R**, **Bamforth F**, **Clive D**, **Greiner R**, **Li L**, **Marrie T**, **Sykes BD**, **Vogel HJ**, **Querengesser L.** HMDB: The human metabolome database. *Nucleic Acids Res* 35, Database: D521–D526, 2007. doi:10.1093/nar/gkl923.
70. **Wolf DE**, **Scott BK**, **Millette CF.** The development of regionalized lipid diffusibility in the germ cell plasma membrane during spermatogenesis in the mouse. *J Cell Biol* 103: 1745–1750, 1986. doi:10.1083/jcb.103.5.1745.
71. **World Health Organization.** *Global Status Report on Noncommunicable Diseases 2014*. Geneva, Switzerland: WHO Press, 2014.
72. **World Health Organization.** *Obesity: Preventing and Managing the Global Epidemic*. Geneva: World Health Organization, 2000.
73. **Zalata AA**, **Christophe AB**, **Depuydt CE**, **Schoonjans F**, **Comhaire FH.** The fatty acid composition of phospholipids of spermatozoa from infertile patients. *Mol Hum Reprod* 4: 111–118, 1998. doi:10.1093/molehr/4.2.111.
74. **Zanetti SR**, **Maldonado EN**, **Aveldaño MI.** Doxorubicin affects testicular lipids with long-chain (C_{18}-C_{22}) and very long-chain (C_{24}-C_{32}) polyunsaturated fatty acids. *Cancer Res* 67: 6973–6980, 2007. doi:10.1158/0008-5472.CAN-07-0376.